Modeling and Analysis of the Pumping Threshold Characteristics in One-Color Two-Photon Excited Cs Vapor

Hanghang Yu, Fei Chen, Qikun Pan, Yang He, and Jijiang Xie

***Abstract*— The pumping threshold is an important parameter for laser sources. Limited by the intricate transition mechanism of the one-color two-photon excitation, there has been a shortage of theoretical studies on the pumping threshold characteristics of alkali vapors. Thus, we propose a physical model of the pumping threshold by innovatively combining the coupled wave equation and the rate equation for one-color two-photon excited Cs vapor. To verify the validity of the model, we compare our simulation results with the available experimental data and show that they agree well with each other. By analyzing the main factors influencing the pumping threshold, we find that the cell temperature and frequency detuning of the pumping laser have a decisive impact on the pumping threshold. These results can provide a valuable reference for the selection of appropriate pumping parameters in further experiments.**

***Index Terms*— Pumping threshold, four-wave mixing, two-photon excitation.**

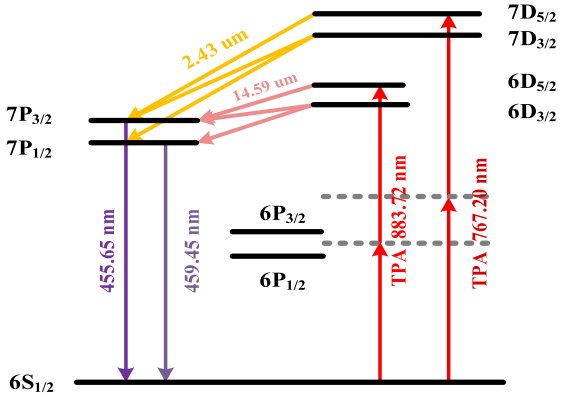

Fig. 1. The energy level diagram and FWM processes for the Cs atom. TPA represents two-photon absorption.

I. Introduction

THE characteristics of the pumping threshold of lasers, especially the intensity threshold, are a flourishing research topic for various types of lasers. In recent years, the parametric four-wave mixing (FWM) process in alkali vapors (mainly Rb and Cs) has demonstrated the potential to realize the generation of lasers with the advantage of achieving a multiwavelength output [1]–[5]. FWM in alkali atoms has been extensively used in various applications, including photon storage [6], [7] and quantum memories [8], the generation of entangled images [9], and the transfer of trans-spectral orbital angular momentum [10]. Many studies on the spectral, absorption and light emission characteristics of one- and two-color laser pumping schemes have also been carried out [11]–[14]. However, the studies of the pumping threshold have been confined to experimental measurements with certain parameters. In addition, a theoretical investigation has been absent because of the complicated transition mechanism for the FWM process in alkali vapors. Clearly, a systematical study of the pumping threshold would be of great interest to provide useful assistance in experiments.

In this paper, we build a physical model to study the characteristics of the pumping threshold in a one-color pumping scheme. Then, verifications of the simulation results with the current experimental records are carried out for four common transition processes in Cs vapor. Finally, we explore the relationship between the pumping threshold and relevant parameters such as the temperature, energy level structure, vapor cell length and frequency detuning of the pumping laser, which can offer important guidance for experiments.

II. Description of the Theory

The energy level diagram and FWM processes in Cs vapor are shown in Fig. 1 with four common pumping states. Before establishing the systematic model, it is necessary to analyze the transition process. The atoms are first excited from the $6S_{1/2}$ ground state to the upper states (6D or 7D) by nonlinear two-photon absorption for FWM in Cs vapor. The middle

Manuscript received October 18, 2019; revised December 18, 2019; accepted December 22, 2019. Date of publication December 30, 2019; date of current version January 24, 2020. This work was supported in part by the National Key Research and Development Program of China under Grant 2018YFE0203201, in part by the Open Fund Project of the State Key Laboratory of Laser and Material Interaction under Grant SKLLIM1815, in part by the National Natural Science Foundation of China under Grant 61675200 and Grant 61705219, and in part by the Youth Innovation Promotion Association of CAS under Grant 2017259. *(Corresponding author: Fei Chen.)*

Hanghang Yu is with the State Key Laboratory of Laser Interaction with Matter, Changchun Institute of Optics, Fine Mechanics and Physics, Chinese Academy of Sciences, Changchun 130033, China, and also with the University of Chinese Academy of Sciences, Beijing 100049, China (e-mail: 13021908922@163.com).

Fei Chen, Qikun Pan, Yang He, and Jijiang Xie are with the State Key Laboratory of Laser Interaction with Matter, Changchun Institute of Optics, Fine Mechanics and Physics, Chinese Academy of Sciences, Changchun 130033, China (e-mail: feichenny@126.com; panqikun2005@163.com; heyang_3g@126.com; laserxjj@163.com).

Color versions of one or more of the figures in this article are available online at http://ieeexplore.ieee.org.

Digital Object Identifier 10.1109/JQE.2019.2963074

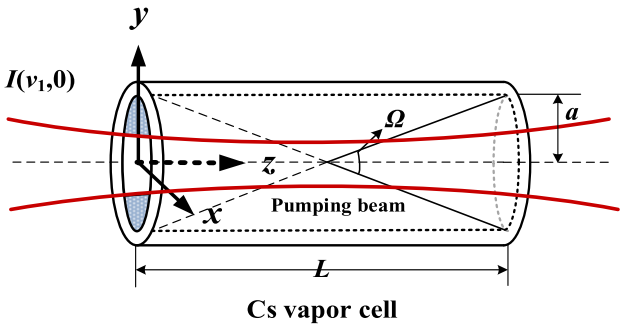

Fig. 2. Schematic diagram of the pumped Cs vapor system.

virtual states marked with the dotted line shown in Fig. 1 are helpful in achieving this process. Afterwards, infrared light is generated from the population inversion between the upper states and 7P state. The three light fields involved in the FWM process are already present. Atoms in the 7P states return to ground state by ultimately radiating coherent blue light. This constitutes a special FWM process with one-color two-photon absorption in Cs vapor.

The original two-photon absorption for FWM in Cs vapor is achieved by the coupling of the two pumping radiation fields. This process does not satisfy the phase matching conditions required for the nonlinear effect. Therefore, the coupled wave equation of two-photon absorption can be used to describe the absorption process. To simplify the calculation, we assume that the incident pumping laser fields are linearly polarized. The coupled wave equation in terms of the electric field intensity of the pumping laser $E(\upsilon_1,z)$ in a one-color pumping scheme can be given by [15]

$$\frac{dE(\upsilon_1,z)}{dz}=\frac{3i(2\pi\upsilon_1)^2}{k_1c^2}\chi_{TA}^{(3)}(\upsilon_1,-\upsilon_1,\upsilon_1)\,|E(\upsilon_1,z)|^2\,E(\upsilon_1,z) \tag{1}$$

where υ_1 is the frequency of the pumping laser and i is the imaginary unit. k_1 is the wavevector. $\chi_{TA}^{(3)}$ is the third-order susceptibility for two-photon absorption. c is the speed of light, and z is the propagation distance of the pumping laser in Cs vapor. $\chi_{TA}^{(3)}$ can be expressed as

$$\chi_{TA}^{(3)}=\frac{N}{6\varepsilon_0h^3}\sum_{k,n,m}\rho_{kk}^0\frac{\mu_{nk}^2\mu_{mn}^2}{(\upsilon_{nk}-\upsilon_1-i\Gamma_{nk})^2(\upsilon_{mk}-2\upsilon_1-i\Gamma_{mk})} \tag{2}$$

where N is the number of Cs atoms per unit volume, and k, n, and m represent the energy states of the 6S, 6P and upper states (6D or 7D states), respectively. υ_{ba} $(a,\ b=k,\ n,\ m)$ represents the transition frequency from state $|b>$ to $|a>$. μ_{ba} $(a,\ b=k,\ n,\ m)$ is the phase relaxation rate. ε_0 is the population occupation probability of the ground state, and ε_0 is the permittivity of vacuum. μ_{ab} corresponds to the dipole moment matrix element of the transition.

Eq. 1 can be transformed according to the relationship between the electric field intensity and power intensity as

$$\frac{dI(\upsilon_1,z)}{dz}=-\frac{3(2\pi\upsilon_1)\mu_0}{n_1^2}\chi_{TA}^{(3)}(\upsilon_1,-\upsilon_1,\upsilon_1)(I(\upsilon_1,z))^2 \tag{3}$$

where μ_0 is the permeability of vacuum and n_1 is the refractive index of the pumping light in Cs vapor. $I(\upsilon_1,\ z)$ is the power intensity of the pumping light with frequency υ_1 at a propagation distance of z. The solution of the above equations based on definite integration can be given as

$$I(\upsilon_1,z)=\frac{I(\upsilon_1,0)}{1+\alpha_1I(\upsilon_1,0)z},\quad \alpha_1=\frac{6\pi}{n_1^2}\mu_0\chi_{TA}^{(3)}\upsilon_1 \tag{4}$$

where $I(\upsilon_1,0)$ is the pumping intensity at the incident surface of Cs vapor cell illustrated in Fig. 2. When the atoms are excited to upper energy states, one should explore the influence of the infrared light on the intensity threshold. Experimental studies have revealed that collimated blue light generation only occurs in the presence of an infrared field [16], [17]. The good correlation between infrared light and blue light means that the pumping threshold of FWM can be acquired by the pumping threshold of the infrared field in Cs vapor.

To accurately calculate the pumping threshold, the rate equation of the infrared photon density, which can describe the generation and propagation processes of the infrared field, is given when the beam diameter remains unchanged along the Cs vapor cell [18]

$$\frac{dN_{IR}}{dt}=\Delta n\sigma_{21}(\upsilon,\upsilon_0)cN_{IR}-\frac{N_{IR}}{\tau_{IR}} \tag{5}$$

where N_{IR} is the infrared light photon density. $\sigma_{21}(\upsilon,\ \upsilon_0)$ and Δn are the emission cross-section and population inversion density between the upper states and the 7P states, respectively. Considering that the population in the 7P states is near zero in the nonexcitation condition, Δn can be considered to be equal to the population density of the upper states (6D or 7D states). The vital parameter τ_{IR} represents the average lifetime of the infrared light photons in the Cs vapor, which can be explained as the time associated with the infrared light photons within a solid angle Ω passing though the vapor cell. This parameter is regarded as the average lifetime of the infrared light photons. According to this physical meaning, τ_{IR} can be defined as

$$\tau_{IR}=\frac{L}{c}\eta \tag{6}$$

where L is the length of the Cs vapor cell and η is the ratio of related solid angle Ω with total value 4π. Ω is calculated relative to the exit end surface and the center of the Cs vapor cell as shown in Fig. 2, which can be approximatively expressed as

$$\Omega=\frac{\pi a^2}{(L/2)^2}. \tag{7}$$

a is the radius of the vapor cell. To realize continual generation and propagation of infrared photons during pumping, Eq. 5 must satisfy

$$\frac{dN_{IR}}{dt}\geq 0. \tag{8}$$

The population inversion density threshold for the upper energy states can be obtained from Eqs. 5 and 6:

$$\Delta n_{th}=\frac{1}{\sigma_{21}(\upsilon,\upsilon_0)\eta L}. \tag{9}$$

For a one-color laser pumping scheme, a pulsed laser is generally used as a pumping source to provide a high pumping intensity, and the pulse width τ_P used in experiments is significantly smaller than the lifetime of the upper states. Thus, the effect of spontaneous radiation can be neglected during the pulsed excitation period. The required intensity threshold for the generation of infrared light during the pulsed excitation time τ_P can be calculated as

$$I_{IRth} = \frac{h\upsilon_{mk}\Delta n_{th}V}{\tau_P S} \tag{10}$$

where $h\nu_{mk}$ is the transition energy from the ground state to the upper state, and V is the volume of the Cs vapor. S is the mode area of the pumping laser. I_{IRth} is the required intensity threshold for the generation of infrared light from the upper state, which can be approximately regarded as the value of absorbed pumping intensity $I(\upsilon_1, L)$ assuming that the mode area of the pumping laser keeps invariance in Cs vapor.

$$I_{IRth} = I(\upsilon_1, L). \tag{11}$$

Therefore, the intensity threshold for FWM can be obtained by substituting Eq. 11 into Eq. 4

$$I_{th}(\upsilon_1, 0) = \frac{I_{IRth}}{2} + \sqrt{(\frac{I_{IRth}}{2})^2 + \frac{I_{IRth}}{\alpha_1 L}}. \tag{12}$$

α_1 is the absorption coefficient shown in Eq. 4. From Eq. 11, we can see that many parameters have an impact on the intensity threshold.

III. Result and Discussion

The common absorption processes for FWM in Cs vapor are the transitions $6S_{1/2}$-$7D_{3/2,5/2}$ and $6S_{1/2}$-$6D_{3/2,5/2}$; through these transitions, we validate the correctness of the physical model.

A. Transition Process of $6S_{1/2}$-$7D_{3/2}$

For the transition $6S_{1/2}$-$7D_{3/2}$, most of the experimental parameters used in the model are shown in Table I. The experimental records and simulation results are plotted in Fig. 3. In Fig. 3(a), the experimental data [19] are reproduced with additional fitting to acquire the energy threshold in the FWM process at two different temperatures. Meanwhile, one can examine the validity of the theory with changes in the temperature. The pumping intensity threshold calculated by our model is obtained for temperatures from 400 K to 500 K in Fig. 3(b). The frequency detunings of the pumping laser and infrared light are set to 1 GHz and zero Hz, respectively, according to the instrument parameters mentioned in Ref. 15. The two special dots in Fig. 3(b) are shown to match the experimental data in Fig. 3(a). The energy thresholds at the two different temperatures in Fig. 3(a) are approximately 1.5 mJ and 2.5 mJ. Correspondingly, the intensity thresholds are approximately 0.97×10^{10}W/m^2 and 1.62×10^{10}W/m^2. From Fig. 3(b), the theoretical results are 0.86×10^{10}W/m^2 and 1.36×10^{10}W/m^2, respectively. By comparison, we can see that the simulations agree well with the experimental data within the permitted error. The error is mainly from measurement error, numerical error in the experiment and parameter error in the simulation results.

TABLE I
MAIN EXPERIMENTAL PARAMETERS CALCULATED IN THE PHYSICAL MODEL

Parameter	Parameter description	Parameter value	
		$6S_{1/2}$-$7D_{3/2}$	6S-$7D_{5/2}$
T	Cell temperature	448 K and 473 K	473 K
λ_{pump}	Wavelength of pumping laser	767.82 nm	767.20 nm
λ_{IR}	Wavelength of infrared light	2.44 μm	2.43 μm
$\Delta\nu_p$	Frequency detuning of pumping laser	1×10^9 Hz	1×10^9 Hz
S	Mode area of pumping laser	3.85×10^{-5} m^2	1.8×10^{-6} m^2
τ_p	Pulse width of pumping laser	4 ns	2.5 ns
a	Radius of vapor cell	2.5 cm	2.5 cm
L	Length of Cs vapor	5 cm	10 cm

In addition, the experimental data can validate the correctness of our model at different temperatures. In the experiment, the ratio of the intensity thresholds $I_{175°C}/I_{200°C}$ is approximately 1.67. The ratio in the simulation result is calculated to be 1.58, which can effectively prove the correctness of the model. The relationship between the intensity threshold and temperature is shown in Fig. 3(b). We can see from Fig. 3(b) that the intensity threshold and temperature exhibit an approximately reciprocal relationship. As the temperature increases, the intensity threshold gradually decreases, and the rate decreases at high temperatures. According to our physical model and the expression of third-order susceptibility for two-photon absorption, the influence of temperature on the intensity threshold is mainly reflected in the population density of the Cs atoms and energy level linewidth. However, the atoms density increases exponentially and energy level linewidth grows in square root with the rise of temperature in a certain range, so the impact of the population density on the intensity threshold is obvious and dominant. Therefore, the intensity threshold has a negative exponential relation with temperature illustrated in Fig. 3(b). The Cs atom density in vapor cell is saturated at approximately 550 K, which means the Cs atom density growth slowly with temperature. This may be the reason for the saturation curve shown in Fig. 3(b).

The intensity threshold versus the frequency detunings of the pumping laser and infrared light at different temperatures is illustrated in Fig. 4. In Fig. 4(a), the intensity threshold increases approximately linearly with an increase in the frequency detuning of the pumping laser. Thus, a high wavelength precision contributes to decreasing the pumping intensity threshold. We can also see that the growth rates are reduced as the temperature increases, so an effective way to

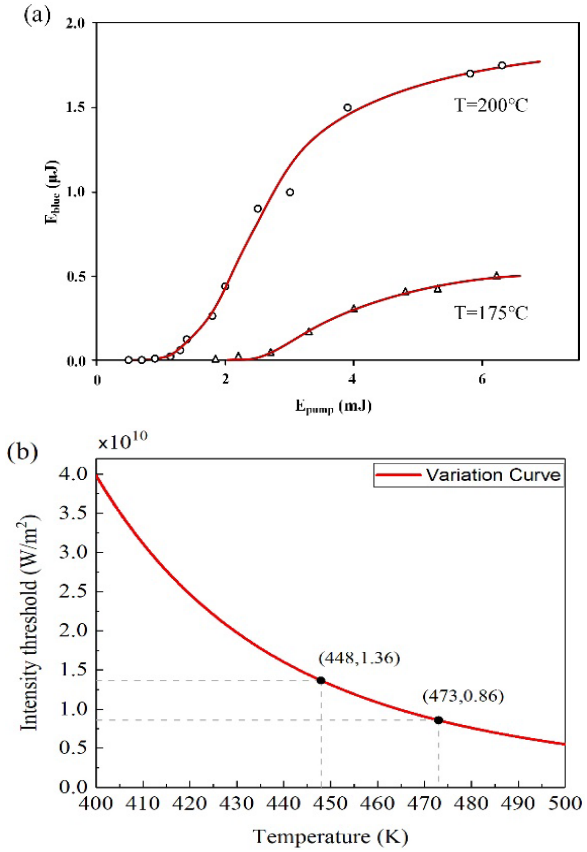

Fig. 3. The experiment records (a) are reproduced with additional fitting. The x-axis is the energy of pumping laser (unit: mJ) and the y-axis is the energy of generated blue light (unit: nJ). The simulation results (b) are obtained when the temperature ranges from 400 K to 500 K. Two special dots are marked for T= 175° and 200°.

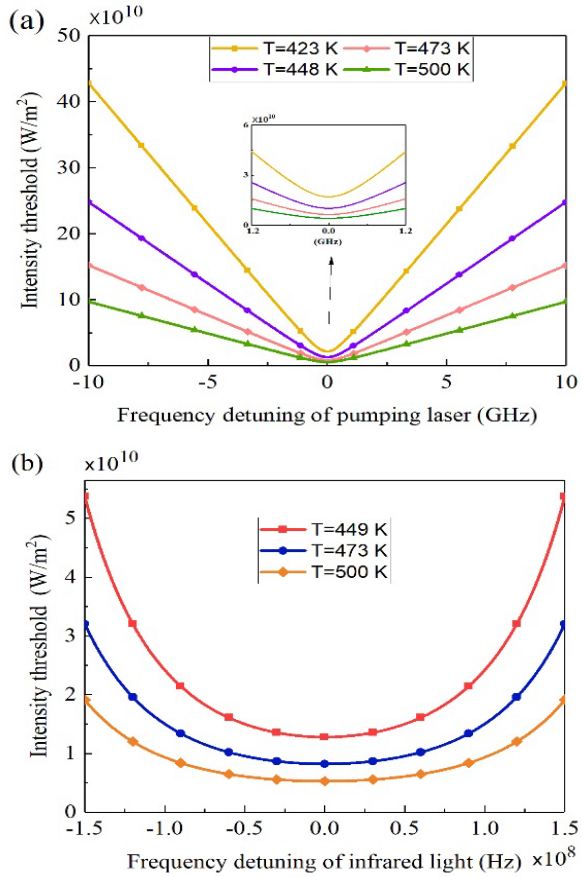

Fig. 4. The intensity threshold versus the frequency detuning of the pumping laser in Fig. 4(a) and the frequency detuning of the infrared light in Fig. 4(b) at different temperatures. (a) The frequency detuning of the infrared light is zero. (b) The frequency detuning of the pumping laser is 1 GHz.

reduce the intensity threshold is to increase the temperature appropriately. The domain of the frequency detuning for the infrared light in Fig. 4(b) has a relation with the Gaussian linewidth between the energy states and frequency detuning of pumping laser. The Gaussian linewidth is about 0.3 GHz with temperature 473 K. The intensity threshold gradually changes with frequency detuning of infrared light within Gaussian linewidth. The reason is that the main influence of frequency detuning of pumping laser is absorption process of two-photon rather than detuning of infrared light. When the frequency detuning of infrared light beyond this range, it is controlled by detuning of pumping laser. It makes intensity threshold increasing exponentially with detuning of infrared light. Similar to Fig. 3(a), the cell temperature has a great effect on the pumping intensity threshold. It can be seen that the intensity threshold has a high tolerance to the frequency detuning of the infrared light in the range of the Gaussian linewidth, which is helpful for achieving phase matching in FWM.

B. Transition Process of $6S_{1/2}$-$7D_{5/2}$

To further verify the correctness of the model, a theoretical simulation for another transition process, $6S_{1/2}$-$7D_{5/2}$, shown in Fig. 5 is carried out. The parameters in the model are set according to the experimental data in Table I. The marked dot in Fig. 5(a) represents the simulation intensity threshold at T = 473 K when the frequency detuning of the pumping laser is 0.5 GHz on the basis of instrument parameters. The simulation result is 2.18×10^{10}W/m^2. This value is close to the experimental result 2.05×10^{10}W/m^2, which is calculated for an energy threshold of 0.09 mJ [20]. This comparison can further prove the validity of our model in characterizing the pumping threshold. In Fig. 5(b), the intensity threshold versus the frequency detuning of the pumping laser at different temperatures exhibits similar features as in Fig. 4(a) because they are only different in terms of the energy state parameters. However, the influence of the frequency detuning of the pumping laser on the intensity threshold is much greater than that in Fig. 4(a).

We also study the relationship between the frequency detunings of the pumping laser and infrared light to discover he regularity of the variation when the pumping intensity is set to a fixed value. In fact, the curves in Figs. 5(c) and 5(d) represent the boundary at which the threshold conditions are satisfied, which means that all the points below the curve can achieve a transition process for the given parameters. Therefore, the difficulty of achieving the FWM process can be expressed as the size of the area below the curve. The influence of temperature on the FWM process is greater than that of the pumping intensity, so an effective way to

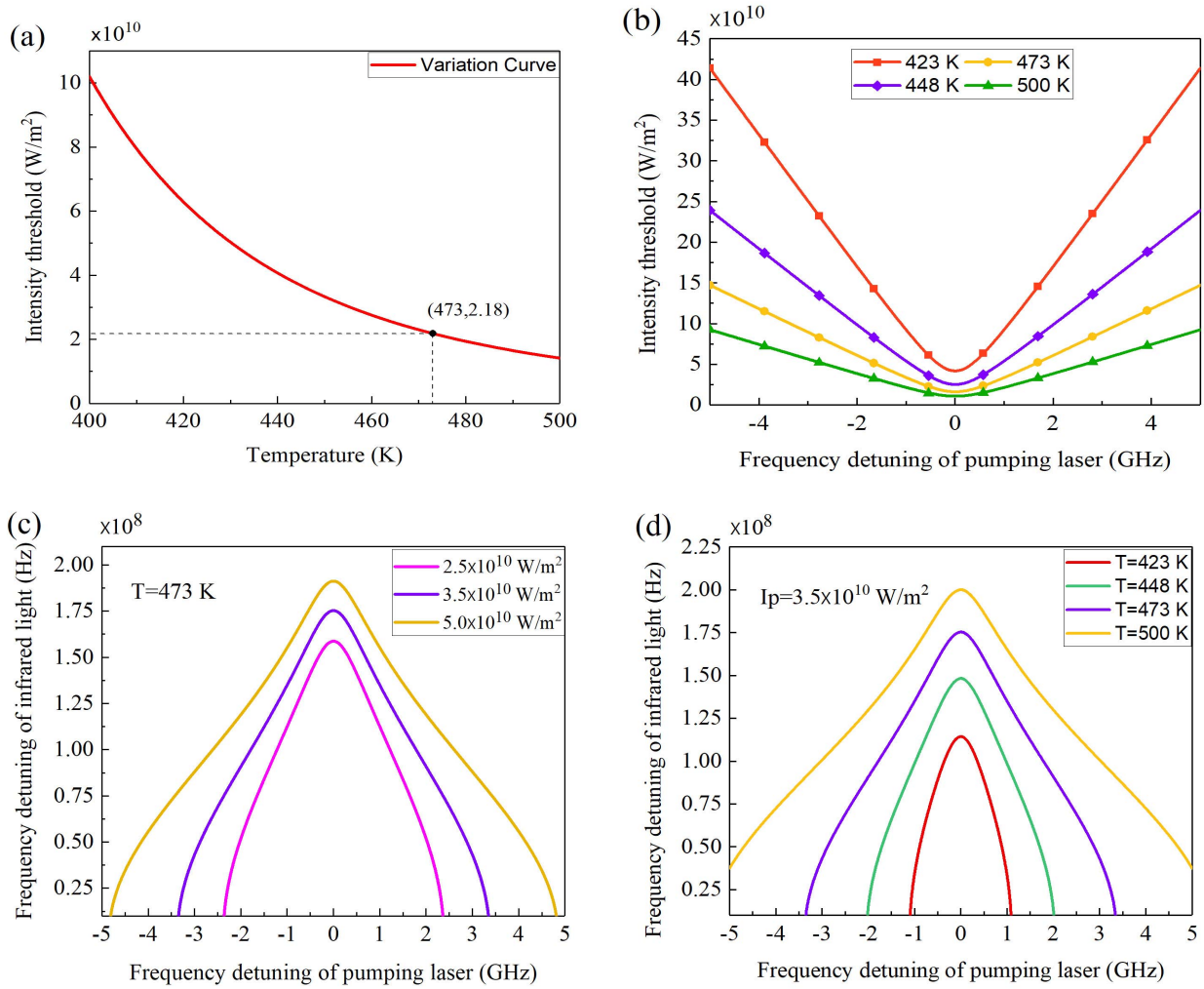

Fig. 5. Simulation results for the transition process $6S_{1/2} - 7D_{5/2}$. (a) The intensity threshold versus the temperature of the Cs vapor. The marked point is used for a comparison with experimental data. (b) The intensity threshold versus the frequency detuning of the pumping laser at different temperatures. (c) The relationship between the frequency detunings of the pumping laser and infrared light at T = 473 K when the pumping intensities are different. (d) The relationship between the frequency detunings of the pumping laser and infrared light at different temperatures when the pumping intensity is constant at Ip $= 3.5 \times 10^{10}$W/m^2.

decrease the intensity threshold is to appropriately increase the temperature. Meanwhile, Figs. 5(a) and 5(d) show that FWM generally requires a high temperature for the transition process $6S_{1/2}$-$7D_{5/2}$.

In addition, the intensity threshold for the transition process $6S_{1/2}$-$6D_{3/2,5/2}$ is also verified. The spontaneous emission rate of the energy states corresponding to infrared light must be considerable for the continue-wave (CW) pumping laser. From the available literature on the $6S_{1/2}$-$6D_{3/2}$ transition, the intensity threshold for the six-wave mixing process (SWM) was discovered as a reference [21]. Our simulation result with the available experimental parameters is 6.37×10^6W/m^2, which is far less than the SWM threshold intensity of 15×10^7W/m^2. This result can indirectly reflect the rationality of our model. In addition, the unattenuated pumping intensity used in absorption spectroscopy of the $6S_{1/2}$-$6D_{5/2}$ transition was approximately 3.2×10^7W/m^2 [22]. The result from our model, referring to vapor cell parameters from the literature, is 1.47×10^7W/m^2, which is consistent with the experimental data considering attenuation. We can see that the intensity threshold for the $6S_{1/2}$-$6D_{3/2,5/2}$ transition is approximately three orders of magnitude smaller than that of the $6S_{1/2}$-$7D_{3/2,5/2}$ transition. The main reason for this result is that the energy difference between the 6P states and virtual states of the $6S_{1/2}$-$6D_{3/2,5/2}$ transition is much less than that of the $6S_{1/2}$-$7D_{3/2,5/2}$ transition. Thus, choosing $6D_{3/2,5/2}$ as upper states has a greater influence.

IV. Conclusion

In this paper, by innovatively combining the coupled wave equation of two-photon absorption and the rate equation, a physical model is established to characterize the pumping threshold in one-color two-photon excited Cs vapor. In this process, the lifetime of the infrared light is reconstructed. Then, a verification of the model is carried out for the transition processes $6S_{1/2}$-$7D_{3/2,5/2}$ and $6S_{1/2}$-$6D_{3/2,5/2}$ according to the available data. The simulation results are in good agreement with the experimental data, which can prove the validity of our model. In addition, we analyze the influences of temperature and the frequency detunings of the pumping laser

and infrared light on the pumping threshold. The frequency detuning of the pumping laser and cell temperature are crucial factors, so two effective ways are proposed to decrease the intensity threshold: increasing the temperature of the Cs vapor as much as possible and improving the wavelength precision of the pumping laser. Our model provides a theoretical method to analyze the characteristics of the pumping threshold in FWM in Cs vapor and will be valuable for the selection of appropriate pumping parameters in experiments.

REFERENCES

[1] J. T. Schultz *et al.*, "Coherent 455 nm beam production in a cesium vapor," *Opt. Lett.*, vol. 34, no. 15, p. 2321–2323, Aug. 2009.

[2] E. Brekke and L. Alderson, "Parametric four-wave mixing using a single cw laser," *Opt. Lett.*, vol. 38, no. 12, p. 2147–2149, Jun. 2013.

[3] A. Majeed *et al.*, "Broadband THz absorption spectrometer based on excitonic nonlinear optical effects," *Light, Sci. Appl.*, vol. 8, no. 1, p. 9, Dec. 2019.

[4] J. F. Sell, M. A. Gearba, B. D. Depaola, and R. J. Knize, "Collimated blue and infrared beams generated by two-photon excitation in Rb vapor," *Opt. Lett.*, vol. 39, no. 3, pp. 528–531, Feb. 2014.

[5] A. M. Akulshin, D. Budker, and R. J. Mclean, "Parametric wave mixing enhanced by velocity-insensitive two-photon excitation in Rb vapor," *J. Opt. Soc. Amer. B, Opt. Phys.*, vol. 34, no. 5, pp. 1016–1022, May 2017.

[6] R. M. Camacho, P. K. Vudyasetu, and J. C. Howell, "Four-wave-mixing stopped light in hot atomic rubidium vapour," *Nature Photon.*, vol. 3, no. 2, pp. 103–106, Feb. 2009.

[7] F. Ripka, Y.-H. Chen, R. Löw, and T. Pfau, "Rydberg polaritons in a thermal vapor," *Phys. Rev. A, Gen. Phys.*, vol. 93, no. 5, May 2016, Art. no. 053429.

[8] A. G. Radnaev *et al.*, "A quantum memory with telecom-wavelength conversion," *Nature Phys.*, vol. 6, no. 11, pp. 894–899, Nov. 2010.

[9] V. Boyer, A. M. Marino, R. C. Pooser, and P. D. Lett, "Entangled images from four–wave mixing," *Science*, vol. 321, no. 5888, pp. 544–547, Jul. 2008.

[10] G. Walker, A. S. Arnold, and S. Franke-Arnold, "Trans–spectral orbital angular momentum transfer via four–wave mixing in Rb vapor," *Phys. Rev. Lett.*, vol. 108, no. 24, Jun. 2012, Art. no. 243601.

[11] T. Efthimiopoulos, M. E. Movsessian, M. Katharakis, and N. Merlemis, "Cascade emission and four–wave mixing parametric processes in potassium," *J. Appl. Phys.*, vol. 80, no. 2, pp. 639–643, Jul. 1996.

[12] Y. Sebbag, Y. Barash, and U. Levy, "Generation of coherent mid-IR light by parametric four-wave mixing in alkali vapor," *Opt. Lett.*, vol. 44, no. 4, pp. 971–974, Feb. 2019.

[13] A. M. Akulshin, R. J. Mclean, A. I. Sidorov, and P. Hannaford, "Coherent and collimated blue light generated by four-wave mixing in Rb vapour," *Opt. Exp.*, vol. 17, no. 25, pp. 22861–22870, Dec. 2009.

[14] W. Y. Cheng and C. M. Wu, "Cesium $6S_{1/2} \rightarrow 8S_{1/2}$ two-photon-transition-stabilized 822.5nm diode laser," *Opt. Lett.*, vol. 32, no. 5, p. 563, 2007.

[15] S. X. Shi, G. F. Chen, W. Zhao, and J. F. Liu, *Nonlinear Optica*, 2nd ed. Shaanxi, China: Xidian Univ., 2012, ch. 5.

[16] A. S. Zibrov, M. D. Lukin, L. Hollberg, and M. O. Scully, "Efficient frequency up-conversion in resonant coherent media," *Phys. Rev. A, Gen. Phys.*, vol. 65, no. 5, pp. 882–886, Jul. 2002.

[17] A. S. Zibrov, "Destruction of darkness: Optical coherence effects and multi-wave mixing in rubidium vapor," in *Proc. AIP Conf. Proc.*, vol. 551, no. 1, pp. 204–217, 2001.

[18] T. S. William, *Laser Fundamentals*, 2nd ed. Cambridge, U.K.: Cambridge Univ., 2004, ch. 4.

[19] C. V. Sulham, G. A. Pitz, and G. P. Perram, "Blue and infrared stimulated emission from alkali vapors pumped through two-photon absorption," *Appl. Phys. B, Lasers Opt.*, vol. 101, nos. 1–2, pp. 57–63, Oct. 2010.

[20] B. Gai *et al.*, "Modulation of a double-line frequency up-conversion process in cesium vapor," *Appl. Phys. B*, vol. 122, no. 6, p. 165, Jun. 2016.

[21] G. P. Perram, N. D. Haluska, and C. A. Rice, "Efficient non-linear two-photon effects from the Cesium 6D manifold," in *Proc. Nonlinear Freq. Gener. Convers., Mater. Devices XVII*, vol. 10516, Feb. 2018, Art. no. 1051606.

[22] T. Ohtsuka, N. Nishimiya, T. Fukuda, and M. Suzuki, "Doppler-free two-photon spectroscopy of $6S_{1/2}$–$6D_{3/2,5/2}$ transition in cesium," *J. Phys. Soc. Jpn.*, vol. 74, no. 9, pp. 2487–2491, 2005.

Hanghang Yu was born in 1992. He received the bachelor's degree from the Shandong Normal University in 2015. He is currently pursuing the degree in optical engineering with the Changchun Institute of Optics, Fine Mechanics and Physics, Chinese Academy of Sciences, China, and the University of Chinese Academy of Sciences, China. He is mainly engaged in the research of alkali metal lasers.

Fei Chen was born in 1982. He received the Ph.D. degree from the Harbin Institute of Technology, in 2011. He is currently with the State Key Laboratory of Laser Interaction With Matter, Changchun Institute of Optics, Fine Mechanics and Physics, Chinese Academy of Sciences. He is currently an Associate Professor and a Doctoral Supervisor. He is mainly engaged in the research of high-power gas lasers and their applications.

Qikun Pan was born in 1985. He received the Ph.D. degree in optical engineering from the Changchun Institute of Optics, Fine Mechanics and Physics, Chinese Academy of Sciences, in 2015. He is currently an Associate Professor. He is mainly engaged in the research of mid infrared laser and their applications.

Yang He was born in 1988. He received the master's degree from Tianjin University, in 2013. He is currently an Assistant Research. He is mainly engaged in the research of solid laser and their applications.

Jijiang Xie was born in 1959. He received the master's degree from the Harbin University of Science and Technology, in 1983. He is currently a Professor. He is mainly engaged in the research of laser and their applications.